doi.org/10.36721/PJPS.2026.39.10.299.1

Berberine ameliorates doxorubicin-induced cardiac toxicity via regulation of the SNHG14/miR-9-5p/PDK4 axis

Qianyun Xu[1,2#], Yuhua Xu[3#] and Hongli Han[4*]

[1]Clinical Medical College, Chengdu University of Traditional Chinese Medicine, Chengdu, China
[2]Hospital of Chengdu University of Traditional Chinese Medicine, Chengdu, China
[3]Jiangsu Health Vocational College, Jiangsu, China
[4]Division of Cardiology, Department of Internal Medicine, Liyuan Hospital, Tongji Medical College, Huazhong University of Science and Technology, Wuhan, China

Abstract: **Background**: Doxorubicin (Dox) has limited clinical application due to its cardiotoxicity. Berberine (Ber) counteracts Dox-induced myocardial injury. **Objectives**: This study uncovers molecular mechanisms through which Ber mitigates Dox-induced myocardial damage by modulating the long non-coding RNAs small nucleolar RNA host gene 14 (SNHG14). **Methods**: To construct Dox-induced cardiotoxicity models in vitro (AC16 cells) and in vivo (male adult rats) for assessing the effects of Ber. Echocardiography was performed to assess the severity of cardiac injury in the rats. RT-qPCR analysis was performed to examine SNHG14 expression. CCK-8, flow cytometry, ELISA and other kits were used to evaluate cell viability, apoptosis, inflammation, oxidative stress and myocardial damage markers. **Results**: Dox boosted SNHG14 and PDK4 in rat myocardial tissues and cultured cardiomyocytes, while suppressing miR-9-5p. Ber reversed the situation, lowering SNHG14 and PDK4 expression and raising miR-9-5p levels. Mechanistically, SNHG14 acts as a miR-9-5p sponge, which leads to the attenuation of miR-9-5p-mediated inhibition of PDK4, ultimately promoting PDK4 expression. The Ber significantly attenuated Dox-induced diastolic dysfunction in rats. It also attenuated apoptosis, inflammation and oxidative stress in AC16 cells; however, this attenuation was substantially reversed by SNHG14, which was partially abolished by miR-9-5p. **Conclusion**: Ber may alleviate Dox-induced cardiac toxicity by inhibiting the SNHG14/miR-9-5p/PDK4 axis and reducing the apoptosis, inflammation and oxidative stress in cardiomyocytes.

Keywords: Doxorubicin; Myocardial damage; SNHG14

Submitted on 29-08-2025 – Revised on 10-11-2025 – Accepted on 20-11-2025

INTRODUCTION

As the incidence of cancer continues to increase, projections suggest that by 2040, there'll be 27 million new cancer cases and nearly 10 million cancer-related deaths each year (Zheng *et al*., 2025a). Anthracycline antibiotics, particularly doxorubicin (Dox) and daunorubicin, are the most frequently prescribed anticancer drugs. However, they are closely associated with cardiotoxicity resulting from cardiomyocyte apoptosis, inflammation and oxidative stress-induced damage (Zou *et al*., 2023). This often manifests as severe and irreversible heart disease, ultimately culminating in left ventricular impairment and heart failure, which significantly hinders the clinical application of Dox (Fujii *et al*., 2024). Several studies have reported berberine (Ber) as a promising agent in clinical research on cardio protection.

Ber, a naturally occurring quinoline alkaloid obtained from the traditional Chinese medical herb *Coptis chinensis* (Huang Lian), has diverse pharmacological effects, including antibacterial, anti-inflammatory, antidiabetic and antitumor activities (Chen and Mao, 2024). Some studies have validated the ability of Ber to counteract cardiac aging via antioxidant and anti-apoptotic actions (Li *et al*., 2022). Recently, pretreatment with Ber was reported to ameliorate diastolic dysfunction in heart failure rats (Mu *et al*., 2025). Moreover, Ber-loaded nano-preparations can ameliorate Dox-induced inflammation in cardiomyocytes *in vitro* (Rawal *et al*., 2022). A recent study revealed that Ber can mitigate myocardial injury by limiting the apoptosis of cardiomyocytes (Wang *et al*., 2023). However, the molecular mechanisms by which Ber alleviates Dox-induced myocardial injury need to be elucidated.

Long non-coding RNA (LncRNA), a subclass of non-coding RNAs (ncRNAs), increases mRNA levels by sponging miRNAs (Wei *et al*., 2025) and plays a pivotal role in cardiac development, function and conditions such as Dox-induced cardiotoxicity. For example, lncRNAs GHET1 (Zhai *et al*., 2024), NOARD (Guan *et al*., 2023) and OXCT1-AS1 (Chen *et al*., 2024) participate in the regulation of Dox-induced cardiotoxicity. The lncRNA small nucleolar RNA host gene 14 (SNHG14), which is located on human chromosome 15q11.2, is an emerging player in myocardial injury. In cellular models of hypoxia-induced congenital heart disease, SNHG14 levels are elevated, which is associated with apoptosis and oxidative stress in cardiomyocytes (Lu *et al*., 2021). Pentoxifylline alleviates ischemic cardiomyopathy by inhibiting SNHG14

**Corresponding author:* e-mail: Hanhonglihhl202@163.com
#These authors contributed equally and are the co-first authors.

(Abd El-Aziz *et al*., 2021). In contrast, a deficiency in SNHG14 mitigates the Ang II-induced reduction in the size and hypertrophy biomarkers of cardiomyocytes (Long *et al*., 2020). Using the Gene Expression Omnibus (GEO) database, in another study, we identified SNHG14 as a differentially expressed lncRNA in mouse hearts treated with Dox. However, the specific role of SNHG14 in the protective effects of Ber against Dox-induced myocardial injury remains unclear. Based on previous research findings, we hypothesized that Ber might exert cardioprotective effects by modulating SNHG14 to ameliorate Dox-induced myocardial injury. To test this hypothesis, we conducted functional assays for SNHG14 in rat models and *in-vitro* in cell models. We further investigated its downstream molecular mechanisms. Our study offers novel insights into how Ber can alleviate Dox-induced myocardial injury.

MATERIALS AND METHODS

Origin of data and detection of genes with differentially expressed lncRNAs (DElncRNAs)

DElncRNAs were identified from the normalized GSE207737 dataset (included in this dataset are heart tissues from C57BL/6J mice injected intraperitoneally with Dox or saline) using the limma package in R. The log2 fold change (log2FC) for each lncRNA was computed directly from the averaged normalized expression values across sample groups. Statistical significance was assessed independently using an empirical Bayes moderated t-test within Limma, with *p-values* adjusted for multiple testing using the Benjamini-Hochberg false discovery rate (FDR) method. LncRNAs with an $|\log2FC| > 1$ and P value < 0.01 were considered statistically significant DElncRNAs.

Cell culture and transfection

Human AC16 cardiomyocytes were maintained in DMEM enriched with 10% FBS and 1% Pen/Strep at 5% CO_2 and a temperature of 37°C. The SNHG14 overexpressing plasmid (oe-SNHG14) and oe-NC were purchased from GenePharma. The plasmids (50 ng) or miR-9-5p mimic oligonucleotides (100 nM) were subsequently mixed with the transfection reagent Lipofectamine 3000 and added to the cells for transfection.

Cell treatment and cell viability

Initially, AC16 cells (1×10^3 cells/well) were treated with different concentrations of Dox, ranging from 0 to 100 μM, for 24 h. To establish a robust model of Dox-induced cardiotoxicity, AC16 cells were treated with 1 μM Dox for 24 h. This concentration was selected as it is approximately 1.6-fold higher than the calculated IC50 value (0.6104 μM, Fig. S1) and reliably induced significant cytotoxicity according to previous research (Chen and Zhang, 2022, Wang *et al*., 2023), thereby providing a clear and consistent injury phenotype for evaluating the protective efficacy of berberine.

Alternatively, these cells were pre-treated with Ber at concentrations ranging from 0 to 8 μM for 24 h, followed by exposure to 1 μM Dox for 24 h according to previous study (Wang *et al*., 2023). The cells were subsequently incubated with DMEM supplemented with the CCK-8 reagent (9:1 ratio) in 37°C incubators. The OD450 nm changes were measured under Automated multimode microplate reader (catalog no. 1912001805, TECAN Spark).

RT-qPCR assay

After obtaining total RNA from cellular samples or tissues with TRIzol. RNA concentrations were subsequently assessed using the Nanodrop 2000c spectrophotometer (catalog no. ND-2000, Thermo Fisher Scientific). Next, 500 ng of cDNA was reverse transcribed into cDNA using the Fastking gDNA Dispelling RT SuperMix kit (for lncRNAs or genes; catalog no. KR118-02, Tiangen Biotechnology Co.) and the miRCute Plus miRNA First-Stand cDNA Synthesis Kit (for miRNA; catalog no. KR211-02, Tiangen Biotechnology Co.). SuperReal PreMix Plus (SYBR Green, for mRNA; catalog no. FP205-02, Tiangen Biotechnology Co.) for mRNA and a miRcute plus miRNA qPCR kit (for miRNAs; catalog no. FP401, Tiangen Biotechnology Co.), employing specific primers and cDNA templates, were used for RT-qPCR in the CFX96 Touch Real-Time PCR Detection System (catalog no.4367659, Thermo Fisher Scientific). U6 served as the internal control for miRNA, while GAPDH was used for lncRNA. Relative expression was calculated using the $2^{-\Delta\Delta CT}$ analytical approach based on three independent biological replicates.

Apoptosis assay

After treatment with Dox, Ber, or transfection with different plasmids, AC16 cells were digested with ethylenediaminetetraacetic acid (EDTA)-free trypsin. After being rinsed with pre-chilled phosphate-buffered saline (PBS), the cells were resuspended in an appropriate binding buffer and then harvested via centrifugation. Next, the cells were stained with a mixture containing 3 μL each of propidium iodide (PI) and Annexin V-fluorescein isothiocyanate (FITC) reagent for a duration of 5 min. Subsequently, the proportion of apoptotic cells was quantified by conducting flow cytometry analysis under flow cytometry (catalog no. 338960, BD FACS Canto II).

Enzyme-linked immunosorbent assay (ELISA)

The concentrations of tumor necrosis factor-α (TNF-α), interleukin-6 (IL-6) and Interleukin-1β (IL-1β), as well as those of myocardial injury markers including cardiac troponin T (cTnI), creatine kinase MB isoenzyme (CK-MB) and lactate dehydrogenase (LDH), were assessed using a commercially available ELISA kit. Cell supernatants, rat serum, or myocardial tissue lysates were collected. Then, 100 μL of each dilution was added to the antibody-coated

plates and incubated. Freshly diluted 0.1 mL of secondary antibody was then added to the well and incubated for 1 h. The wells were washed and the OD450 nm was measured after adding the termination solution under Automated multimode microplate reader (catalog no. 1912001805, TECAN Spark).

Siperoxide dismutase (SOD) and malondialdehyde (MDA) assay

We determined the levels of MDA and the activity of SOD in the cells. For assessing SOD activity, the reagents provided in the kit were prepared and then combined with the harvested cells. The mixture was vortexed and incubated at 37ºC for 40 min. Subsequently, 2 mL of the chromogenic reagent was added to the mixture, which was then allowed to equilibrate at room temperature for 10 min and the OD550 was recorded.

To determine MDA levels, the reagents were meticulously prepared and then added to the cell samples. These samples were subsequently incubated in a water bath maintained at 95ºC for 40 min. After incubation, the samples were rapidly cooled under a stream of running water and then centrifuged at 3500 rpm for 10 min. The resulting supernatant was used for measuring the OD532 under Automated multimode microplate reader (catalog no. 1912001805, TECAN Spark).

Extraction of subcellular fraction

After harvesting AC16 cells, RNA was isolated with a PARIS kit (AM1921, Life Technologies). Next, the levels of SNHG14 in the cytoplasmic and nuclear compartments were quantified by conducting RT-qPCR analysis. U6 served as the internal reference gene for the nuclear fraction, whereas GAPDH was used as the internal reference for the cytoplasmic fraction.

Bioinformatics analysis

The target miRNAs of SNHG14 were identified through predictive analysis by accessing the ENCORI, DIANA and miRDB databases. The overlapping target miRNAs were subsequently mapped by the bioinformatics online platform. The targets of miR-9-5p were identified by conducting a comprehensive predictive analysis by accessing multiple bioinformatics databases, including the TargetScan, miRDB, ENCORI, miRPathDB and microT-CDS databases. The targets of Dox and Ber were downloaded from the CDT databases.

Dual luciferase reporter (DLR) assay

The 3'-UTR segments of SNHG14 and pyruvate dehydrogenase kinase 4 (PDK4), each encompassing a binding site for miR-9-5p, along with their corresponding mutant forms, were chemically synthesized and subsequently cloned and inserted into the luciferase reporter vector pmirGLO. This process led to the generation of four recombinant luciferase reporter constructs, including SNGH-WT (wild-type), PDK4-WT, SNHG14-MT (mutant) and PDK4-MT. Next, AC16 cells were seeded, and the plasmids were separately co-transfected with the miR-9-5p mimic/inhibitor and their respective negative controls using a transfection reagent. After incubation for 48 h, both firefly and Renilla luciferase activities were examined.

RNA immunoprecipitation (RIP) assay

A Magna RIP RNA-binding protein immunoprecipitation kit was used. Next, the Argonaute 2 (Ago2) antibody or negative control immunoglobulin G (IgG) antibody was mixed with magnetic beads, supplemented with the cell lysate and incubated overnight at 4ºC. After treatment with proteinase K, RNA was extracted by RT-qPCR.

Animals and groups

This study complied with the "Guide for the Care and Use of Laboratory Animals" and conformed to the ARRIVE Guidelines. All animal-related procedures and experimental protocols were performed strictly following regulations implemented by the Research Ethics Committee of Chengdu University of Traditional Chinese Medicine (No.2018-01-0213). A sample size of 80 rats (n = 8/group) was found to provide 80% power with a 95% confidence interval and 5% significance level using the G*Power program. To prevent rat deaths during the experiment from affecting the results, we used n = 10 rats per group.

Male Sprague-Dawley rats weighing 180 g-220 g (n = 100) were obtained from Beijing Viton Lihua Laboratory Animal Technology Co., Ltd., Shanghai branch (SCXK 2022-0007). All rats were housed at standard conditions of 24°C and 50-70% humidity. Rats were group-housed at 5 rats per cage. The assays commenced after seven days of adaptation.

The rats were allocated into two separate cohorts. The initial cohort comprised 50 rats, which were randomly assigned to five distinct groups (n = 10, using a randomization tool from the website): the control (0.9% saline), Dox (20 mg/kg Dox), Dox+Ber (20 mg/kg Dox combined with Ber), Dox+Ber+LV-SNHG14 and Dox+Ber+LV-NC groups. A lentiviral control vector LV-NC was purchased from Shanghai GenePharma. These vectors were administered via tail vein injection at a dosage of 5×10^7 UT/50 μL one day before Dox and Ber treatment was initiated. The remaining groups concomitantly received an equivalent volume of saline through the tail vein. Dox and Ber were purchased from Lingnan Pharmaceuticals Co. and Acros Organics, respectively; they were dissolved in 0.9% saline before usage. Following established protocols, the control and Dox groups received 0.9% sailing via gavage daily for 10 days, whereas the other groups received 20 mg/kg Ber via gavage daily for the same period. Additionally, all rats except those in the control group were administered 20 mg/kg Dox intraperitoneally (IP) on days 2, 4 and 6, with the controls receiving Dox via the IP route according to a previous

study (Wu *et al*., 2019). The second batch of rats was specifically used to probe the functions of miR-9-5p. A total of 50 rats were randomly distributed into five groups: Dox+Ber, Dox+Ber+LV-SNHG14, Dox+Ber+LV-NC, Dox+Ber+LV-SNHG14+miR-9-5p agomir and Dox+Ber+LV-SNHG14+agomir NC. On the first day, each rat in the treatment group was injected with 10 nM ribonucleotide (0.2 mL saline), whereas the other rats received only saline.

No deaths occurred during the experiment, and the condition of the rats was monitored. On the tenth day of the experiment, following ultrasound assessment and 30 minutes after the last administration, all rats were euthanized through an intraperitoneal injection of 80 mg/kg pentobarbital sodium. Next, abdominal aorta blood samples were collected from each rat following laparotomy. Serum was obtained via centrifugation at 500×*g* and 4°C. The hearts were promptly exercised, rinsed in chilled saline and preserved in liquid nitrogen.

Echocardiography analysis

Unidentified groups of experimenters scanned rats using a high-resolution VisualSonics Vevo770 *in-vivo* microimaging system (catalog no. 770, VisualSonics lnc. Fujifilm Visual Sonics) with a center frequency of 17.5 MHz on the RMV 707 transducer in a blinded fashion. The rats were placed in the supine position for imaging and cardiac function and the success of the model were assessed by monitoring the left ventricular ejection fraction (LVEF) and left ventricular fractional shortening (LVFS) in M-model echocardiography. Moreover, left ventricular end-diastolic diameter (LVEDD) and left ventricular end-systolic diameter (LVESD) were also measured to further evaluate cardiac structure and function. Additionally, cardiac output (CO) was calculated using the Vevo770 imaging system software, which uses data derived from at least three successive cardiac cycles.

Statistical analysis

All values are presented as the mean ±SD of at least three replicates. Statistical evaluation involved ANOVA, followed by Tukey's post-hoc multiple comparison tests. All statistical computations and data visualization were conducted using GraphPad Prism version 9.0 (Graphapd Software, La Jolla). All results were considered to be statistically significant at $P < 0.05$.

RESULTS

Ber protects against Dox-induced cardiomyocyte injury in-vitro

To elucidate the role of Ber in Dox-induced myocardial injury, we developed an AC16 cell model exposed to different concentrations of Dox. Cell viability decreased progressively as the Dox doses increased ($P < 0.05$, Fig. 1A). Pretreatment with 0.5, 1, 2, or 4 μM concentrations markedly attenuated the detrimental impact of 1 μM Dox on the cell ($P < 0.05$, Fig. 1B). As shown in Fig. 1B, Ber exhibits optimal and stable protective efficacy within the 0.5-1 μM range. At concentrations ≥ 2 μM, the protective efficacy tends to plateau or even diminish. In summary, this study employed 1 μM Ber for experimentation.

Additionally, Dox promoted apoptosis, but Ber significantly reversed this effect ($P < 0.05$, Fig. 1C). Ber decreased MDA levels and increased SOD expression ($P < 0.05$, Fig. 1D) and partially negated the overproduction of IL-1β, IL-6 and TNF-α in AC16 induced by Dox (Fig. 1E). Dox significantly increased the levels of CK-MB, cTnI and LDH; however, this increase was significantly attenuated by Ber ($P < 0.05$, Figs. 1F-H). The GEO database analysis revealed that SNHG14 was significantly upregulated during Dox-induced myocardial injury, with a 9.32-fold increase in expression (Fig. 1I). Dox-stimulated AC16 cells presented high SNHG14 levels, which were noticeably suppressed by Ber ($P < 0.05$, Fig. 1J).

SNHG14 overexpression counteracts Ber's mitigation of dox-induced myocardial injury

To elucidate the functional contribution of SNHG14 to Ber-modulated cardiomyocyte injury, we overexpressed SNHG14 in AC16 cells *in-vitro* via transfection with oe-SNHG14 plasmids. We found that Ber weakened the increase in SNHG14 levels induced by Dox, but transfection with oe-SNHG14 significantly restored the expression of SNHG14 (Fig. 2A). Moreover, the restoration of the viability of AC16 cells by Ber was notably diminished by the increase in SNHG14 levels ($P < 0.05$, Fig. 2B). The ability of Ber to suppress apoptosis was markedly reduced as SNHG14 levels increased ($P < 0.05$, Fig. 2C). Moreover, the increases in SNHG14 mitigated the suppressive effect of Ber on MDA, IL-1β, TNF-α and IL-6 levels and reduced the promotion of SOD in Dox-induced AC16 cells (Figs. 2D-E). The increase in SNHG14 levels increased CK-MB, cTnI and LDH and limited the cardioprotective role of Ber against cardiomyocyte injury ($P < 0.05$, Figs. 2F-H).

MiR-9-5p is a molecular sponge for lncRNA SNHG14

To further elucidate the mechanism of SNHG14 in Ber resistance to Dox-induced myocardial injury, we assessed the subcellular localization of SNHG14. We found that SNHG14 was located primarily in the cytoplasm (Fig. 3A). Bioinformatics prediction identified miR-9-5p as an overlapping target miRNA of SNHG14 (Fig. 3B). The binding sequences between them are shown in Fig. 3C. Moreover, the overexpression of miR-9-5p considerably inhibited the luciferase activity of SNHG14-WT than the mimic NC, whereas no notable change was observed in SNHG14-MT (Fig. 3D). SNHG14 and miR-9-5p are enriched mainly in Ago2 ($P < 0.05$, Fig. 3E). Moreover, Ber decreased the repression of miR-9-5p levels by Dox, but this decrease was noticeably reversed by the overexpression of SNHG14 ($P < 0.05$, Fig. 3F).

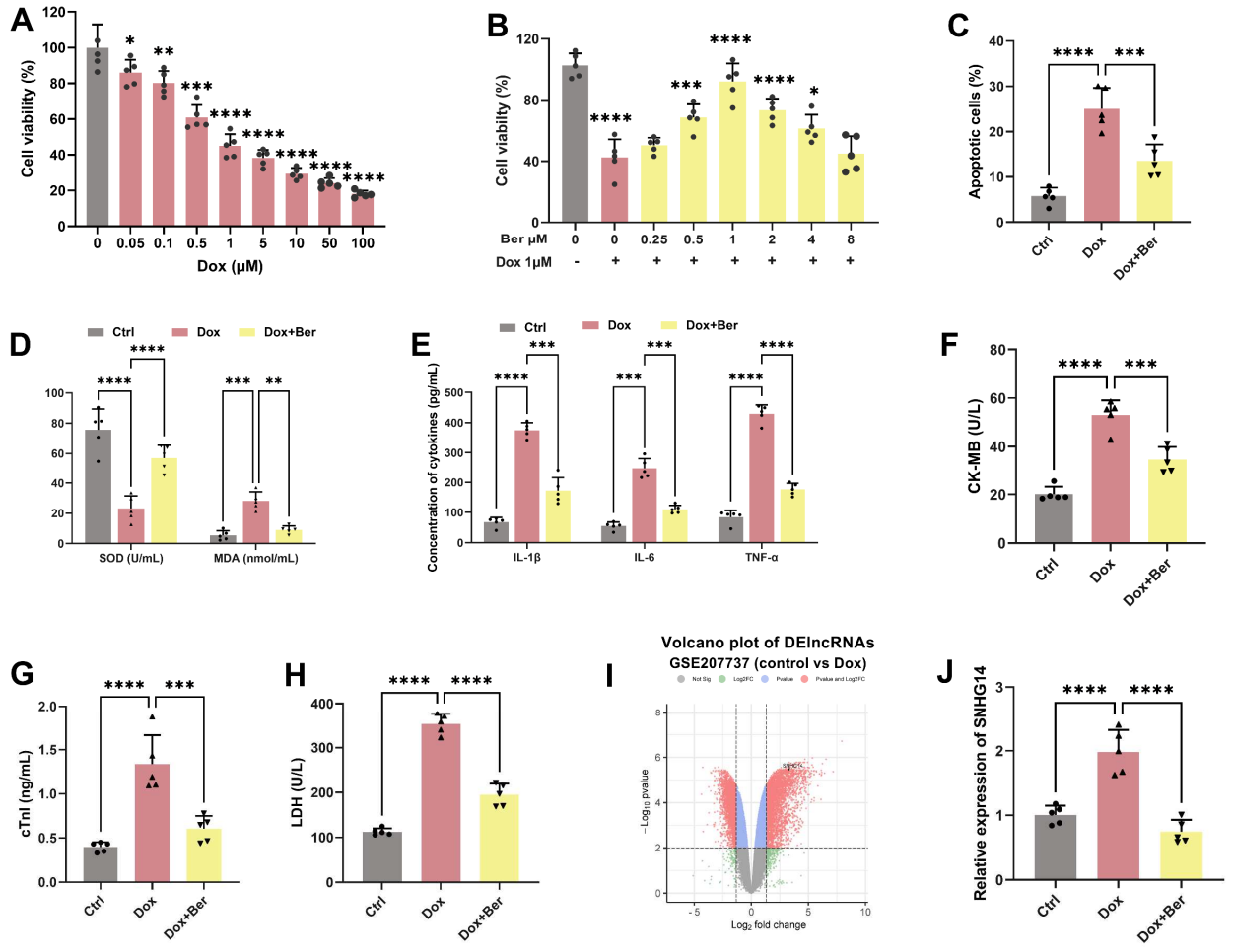

Fig. 1: Ber can alleviate Dox-induced cardiomyocyte stress, oxidative stress, and inflammation *in-vitro*. (A) CCK-8 assay was conducted to assess changes in the viability of AC16 cells after stimulation with different concentrations of Dox or; (B) with different concentrations of Ber; (C) The percentage of apoptotic cells was detected by flow cytometry; (D) The levels of oxidative stress indices SOD and MDA were determined using commercial kits; (E) Secretion of inflammatory factors in the supernatant of AC16 cells was detected by ELISA; (F) Commercial test kits were used to analyze the levels of the myocardial injury markers CK-MB; (G) cTnI and; (H) LDH; (I) Volcano plot of the GEO database identifying differentially expressed lncRNAs associated with Dox-induced myocardial injury; (J) The effects of Ber and Dox on SNHG14 in AC16 cells were detected by RT-qPCR. The data were shown as mean ± SD, n = 5 in each group, *$P < 0.05$, **$P < 0.01$, ***$P < 0.001$, ****$P < 0.0001$.

SNHG14 eliminates the cardioprotective effect of ber against dox-induced cardiomyocyte injury by targeting miR-9-5p

To verify the protective role of SNHG14/miR-9-5p in cells against Dox-triggered myocardial injury, we introduced miR-9-5p mimics into SNHG14-expressing cells following Ber pretreatment and Dox exposure. The results revealed a significant rebound in miR-9-5p levels ($P < 0.05$, Fig. 4A). Moreover, SNHG14 reduced Ber-induced cell viability and increased apoptosis, but these effects were significantly reversed by the overexpression of miR-9-5p (Figs. 4B-C). Additionally, the increase in SNHG14 decreased the antioxidant stress and anti-inflammatory effects mediated by Ber, both of which were significantly restored by the overexpression of miR-9-5p (Figs. 4D-E). The upregulation of miR-9-5p effectively counterbalanced the stimulatory effects of SNHG14 on the levels of CK-MB, cTnI and LDH in AC16 cardiomyocytes subjected to Ber treatment ($P < 0.05$, Figs. 4F-H).

SNHG14 over-expression weakens Ber's in vivo protection against dox-triggered cardiac diastolic dysfunction, oxidative stress and inflammation

To comprehensively elucidate the functional role of SNHG14, we conducted a series of experiments in which we deliberately modulated its expression within a rat model of myocardial injury induced by Dox and subsequently treated with Ber as illustrated in Fig. 5A. Dox treatment led to a significant upregulation of SNHG14 expression in the myocardial tissues of rats.

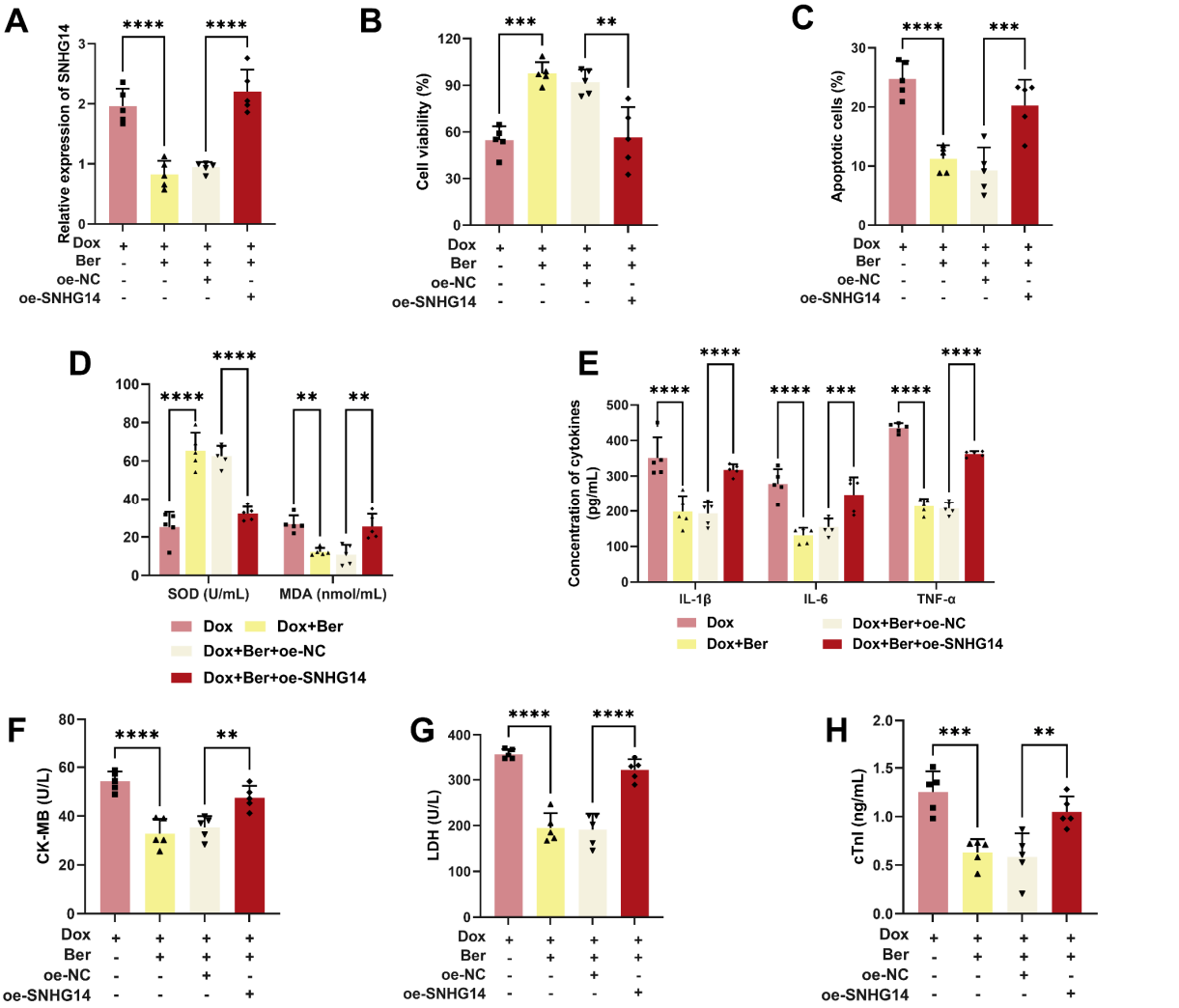

Fig. 2: Overexpression of SNHG14 abolished the cardioprotective, anti-oxidative damage, and anti-inflammatory effects of Ber *in-vitro*. (A) RT-qPCR was performed to detect the expression level of SNHG14 in AC16 cells after the overexpression of SNHG14; (B) Changes in cell viability after overexpression of SNHG14 were determined by a CCK-8 assay; (C) The effect of SNHG14 on apoptosis was analyzed by flow cytometry; (D) Commercial test kits were used to examine the levels of SOD and MDA; (E) The expression levels of inflammatory factors were evaluated by ELISA; (F-H) Commercial test kits were used to detect CK-MB, LDH and cTnI in the cells. The data were shown as mean ± SD, n = 5 in each group, *$P < 0.05$, **$P < 0.01$, ***$P < 0.001$, ****$P < 0.0001$.

Interestingly, this Dox-induced elevation in SNHG14 levels was effectively mitigated by Ber administration. However, when SNHG14 was overexpressed, the mitigating effect of Ber was completely reversed, with statistical significance ($P < 0.05$, Fig. 5B). Dox also impaired cardiac function, as indicated by suppressed CO, LVEF and LVFS, along with increased LVEDD, LVESD and serum CK-MB levels. Ber treatment reversed these changes, but this protective effect was abolished by SNHG14 overexpression ($P < 0.05$, Figs. 5C-F and Fig. S2). Furthermore, Dox induced oxidative stress and inflammation, as indicated by MDA levels and the secretion of IL-1β, IL-6 and TNF-α, along with suppressed SOD levels in rat myocardial tissues. However, Ber significantly alleviated these effects. In contrast, the upregulation of SNHG14 exacerbated these effects ($P < 0.05$, Figs. 5G-I).

MiR-9-5p partially reversed the abolishment of ber-mediated cardioprotection by SNHG14 overexpression

As depicted in Fig. 6A, in the myocardial tissue of Ber-treated rats with Dox-induced myocardial injury, SNHG14 overexpression lowered miR-9-5p levels. Yet, agomir miR-9-5p notably counteracted this decline. Moreover, miR-9-5p counteracted the inhibitory impact of SNHG14 overexpression on rat CO, LVEF and LVFS, while also reversing its promoting effects on LVEDD and LVESD (Figs. 6B-D and Fig. S3). Finally, upregulation of miR-9-5p partially attenuated the increase in CK-MB levels, oxidative stress and pro-inflammatory factors that were induced by SNHG14 ($P < 0.05$, Figs. 6E-H).

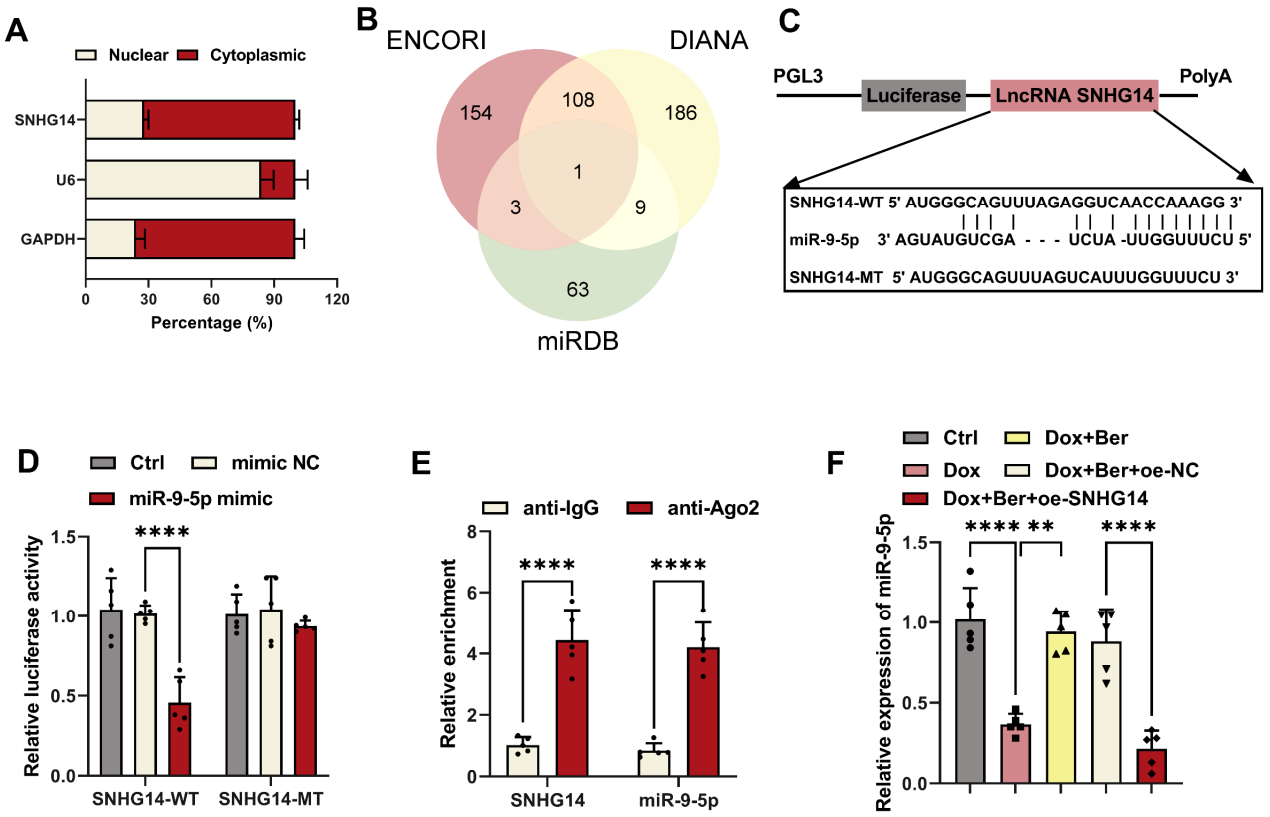

Fig. 3: MiR-9-5p is a target of SNHG14. (A) Subcellular localization analysis of SNHG14; (B) The Venn diagram shows the overlapping target miRNAs predicted by the three databases; (C) Target binding sequences between SNHG14 and miR-9-5p; (D-E) Dual luciferase reporter and RIP assays validated the targeting relationship between SNHG14 and miR-9-5p. (F) RT-qPCR was performed to detect the effects of Dox, Ber, and SNHG14 on miR-9-5p levels in AC16 cells. The data were shown as mean ± SD, n = 5 in each group, *$P < 0.05$, **$P < 0.01$, *** $P < 0.001$, ****$P < 0.0001$.

PDK4 was a target of miR-9-5p

The targets of SNHG14/miR-9-5p in the anti-Dox-induced myocardial injury effects of Ber were further investigated. Multiple databases were used to predict 247 overlapping miR-9-5p target genes (Fig. 7A). By conducting further analyses, we identified four overlapping mRNAs that are also targets of the actions of Ber and Dox, including PDK4 (Fig. 7B). The binding sequence between them is shown in Fig. 7C. The miR-9-5p mimic markedly suppressed the luciferase activity of PDK4-WT (Fig. 7D). SNHG14, miR-9-5p and PDK4 were enriched in association with Ago2 immunoprecipitated (Fig. 7E). Moreover, compared with the control group, Dox elevated PDK4 expression in AC16 cells. Notably, Ber substantially mitigated this effect. Overexpressing SNHG14 reinstated PDK4 levels, yet miR-9-5p attenuated this reinstatement ($P < 0.05$, Fig. 7F).

DISCUSSION

Doxorubicin (Dox) is considered a potent anti-tumor antibiotic; however, clinical evidence indicates a 9% incidence of late-onset congestive heart failure (CHF) among cancer survivors (Linders *et al*., 2024). Hence, new strategies need to be developed to reduce or prevent cardiotoxicity. Several studies have indicated that Ber can decrease the oxidative stress, apoptotic and inflammatory responses induced by Dox, protecting the heart, liver and kidneys, although its exact mechanism of action is unknown (Wang *et al*., 2023, Ahmedy *et al*., 2025). Our study revealed that SNHG14 blocks the protective effects of Ber against Dox-induced cardiac issues, including dysfunction, apoptosis, inflammation and oxidative stress in rats (*in-vivo*) and cells (*in-vitro*). This may be due to the miR-9-5p/PDK4 axis. Our study revealed a new mechanism concerning how Ber alleviates Dox-induced cardiotoxicity.

Dox-induced cardiotoxicity is characterized by excessive inflammation, which is indicated by an increase in the release of pro-inflammatory factors. Ber has anti-inflammatory effects, improving dry eye conditions (Han *et al*., 2023) and alleviating senescence-associated secretory phenotypes related to inflammation in atherosclerosis (Zheng *et al*., 2025b). In our study, Ber decreased the secretion of pro-inflammatory factors in AC16 cells and rat serum. Oxidative stress is another important aspect of Dox-triggered cardiotoxicity. Ber inhibits oxidative stress, thereby reducing atherosclerosis (Zhang *et al*., 2021b), spinal cord injury (Ma *et al*., 2024) and acute hyperlipidemia (Alruhaimi *et al*., 2024).

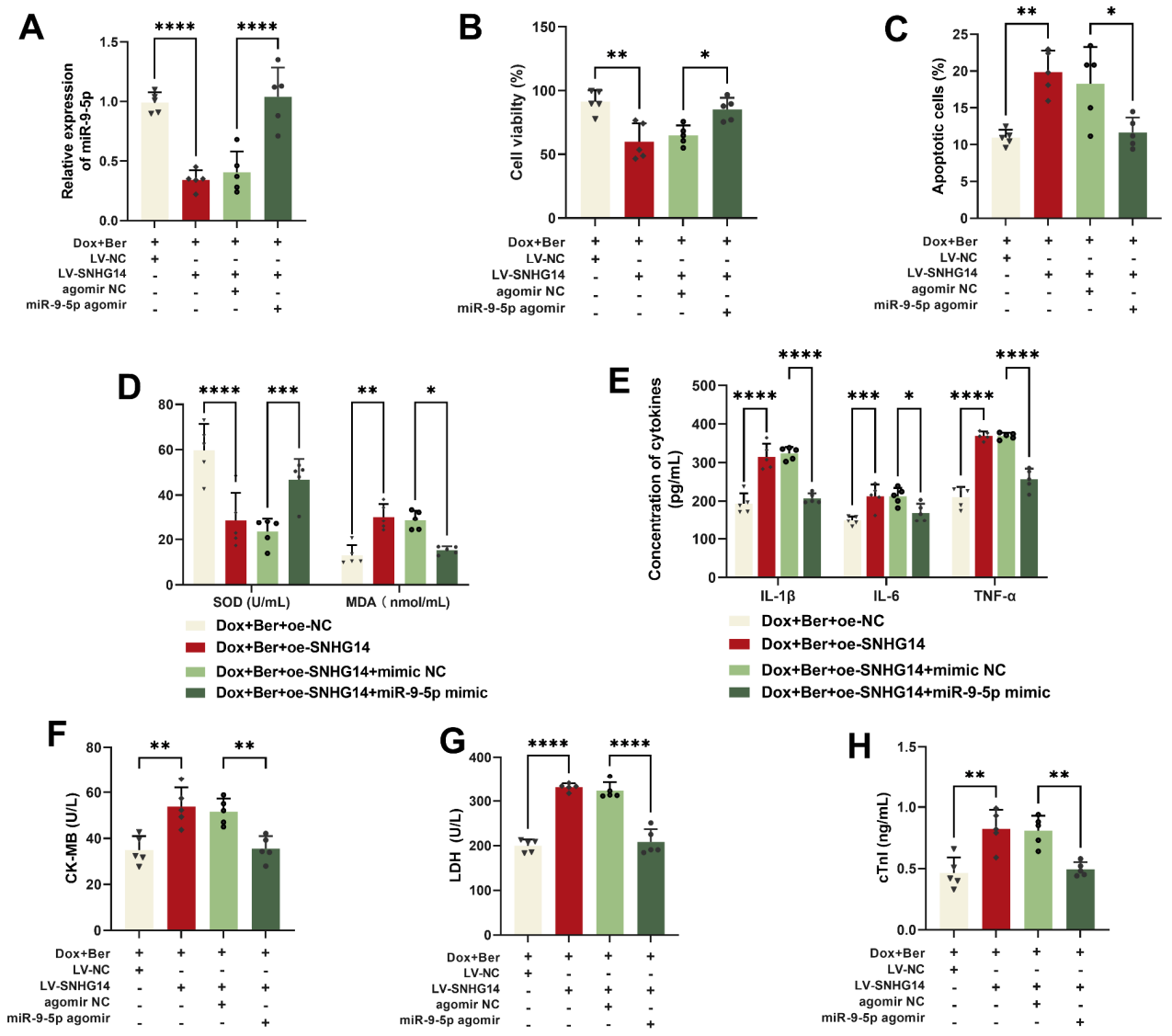

Fig. 4: SNHG14 eliminates the cardioprotective effect of Ber on Dox-induced cardioprotection by targeting miR-9-5p *in vitro*. (A) RT-qPCR was performed to detect miR-9-5p expression in SNHG14 overexpressing cells treated with Ber and Dox. (B) A CCK-8 assay was conducted to examine the viability of cells overexpressing miR-9-5p. (C) Flow cytometry analysis of the effect of miR-9-5p on apoptosis. (D-E) Commercially available assay kits and ELISA were used to analyze the effect of miR-9-5p on oxidative stress indicators and inflammatory factor levels in AC16 cells. (F-H) Commercially available assay kits were used to analyze the levels of the myocardial injury markers cTnI, CK-MB, and LDH in the context of the overexpression of miR-9-5p. The data were shown as mean ± SD, n = 5 in each group, **P* < 0.05, ***P* < 0.01, ****P* < 0.001, *****P* < 0.0001.

Ber has cardioprotective effects, such as relieving myocardial ischemia by dampening inflammatory responses and oxidative stress (Jia *et al*., 2022) and preventing myocardial damage caused by the overactivation of adrenaline (Yang *et al*., 2024). It has been demonstrated that Ber mitigated Dox-induced myocardial injury by eliminating oxidative stress (Wang *et al*., 2023). Consistent with these previous findings, our findings revealed that Ber alleviates Dox-trigged myocardial injury. The lncRNA SNHG14 is associated with inflammation, apoptosis and oxidative stress. It exerts neuroprotective effects on Parkinson's disease through dual modulation of NLRP3 inflammasome-mediated neuroinflammation and oxidative stress (Xu *et al*., 2024); however, it contributes to ischemic brain injury (Zhang *et al*., 2021a). High levels of SNHG14 exacerbate tubular injury in diabetic nephropathy (Huang *et al*., 2025) and promote inflammation and apoptosis in PC-12 cells (Jiang *et al*., 2021). In contrast, knocking down SNHG14 reduces inflammation and apoptosis in lung epithelial cells by restoring the expression of miR-124-3p (Zhu *et al*., 2021).

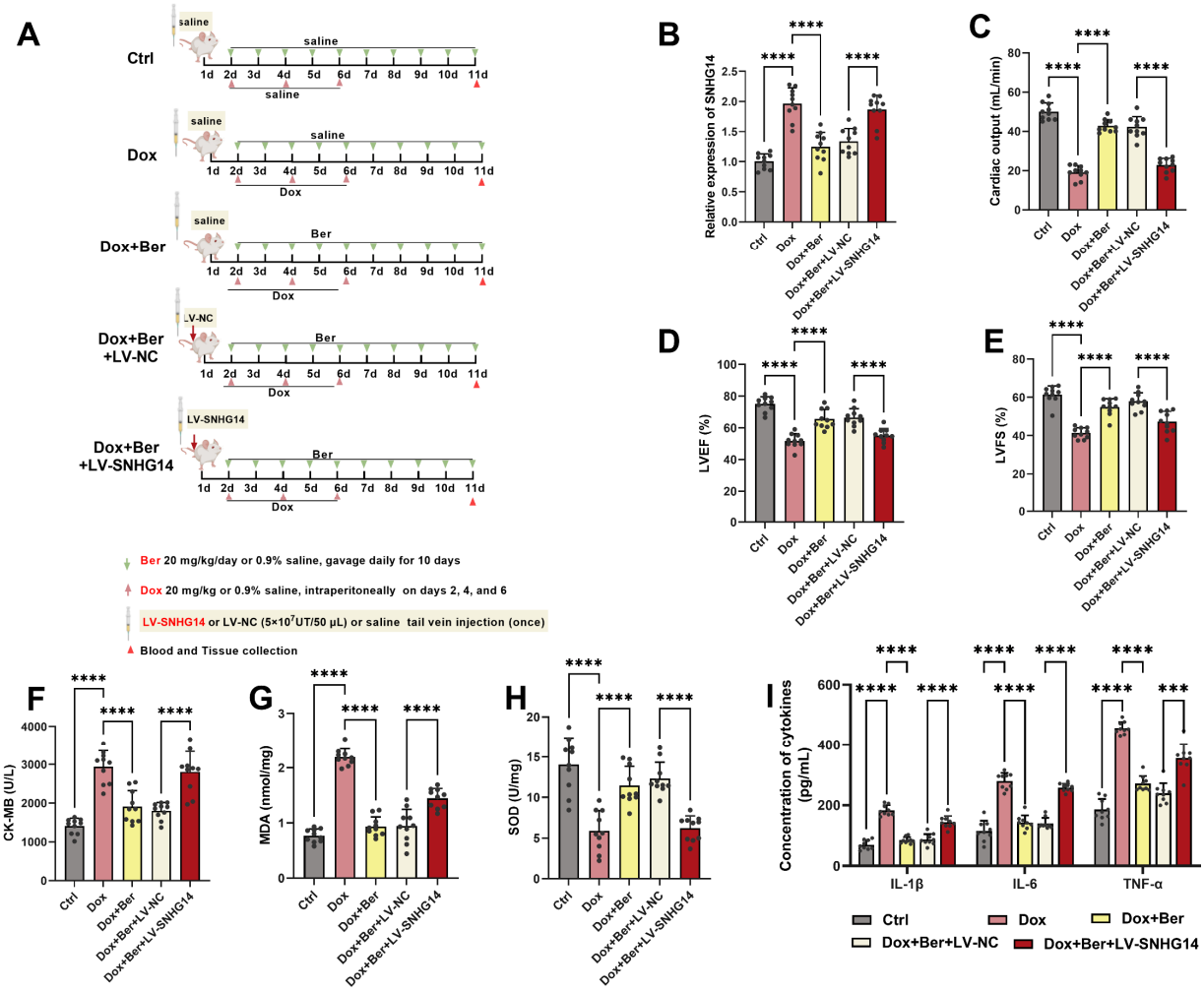

Fig. 5: SNHG14 attenuates Ber-induced cardiac diastolic dysfunction, oxidative stress, and inflammation *in-vivo*. (A) Schematic plans of the rats in the Dox+Ber+LV-SNHG14 groups. (B) The levels of SNHG14 in the myocardium of rats on day 15 were detected by RT-qPCR. (C-E) Echocardiography was used to quantify cardiac output, LVEF, and LVFS. (F) The levels of CK-MB in rat serum were analyzed using a commercial kit. (G-H) The levels of MDA and SOD in myocardial tissues were examined using commercial kits in the myocardium tissues. (I) ELISA was conducted to measure the levels of pro-inflammatory cytokines in the serum of the rats. The data were shown as mean ± SD, n = 10 rats/group, $*P < 0.05$, $**P < 0.01$, $***P < 0.001$, $****P < 0.0001$.

SNHG14 is also involved in myocardial injury. In a mouse model of sepsis-induced myocardial injury, its expression levels increase (Bi *et al*., 2024). Pentoxifylline exerts a cardioprotective effect against myocardial ischemia-reperfusion injury through the suppression of the expression of SNHG14 (Abd El-Aziz *et al*., 2021). Additionally, SNHG14 exacerbates LPS-induced cardiomyocyte injury (Bi *et al*., 2024) and hypoxia-induced H9c2 cardiomyocyte injury by promoting apoptosis and oxidative stress, but silencing SNHG14 attenuates these effects (Lu *et al*., 2021). In our study, we revealed that SNHG14 levels were elevated in Dox-induced myocardial injury. Both *in-vitro* and *in-vivo*, Ber reduced Dox's elevation of SNHG14 and alleviated oxidative stress, apoptosis, inflammation and myocardial dysfunction. Moreover, the overexpression of SNHG14 counteracted the cardioprotective effect of Ber in both Dox-challenged rats and cardiomyocytes. Consequently, our findings suggest that Ber confers protection against Dox-induced myocardial damage by attenuating SNHG14 expression.

LncRNAs generally play a role in disease progression as molecular sponges for miRNAs (Tian and Zhang, 2025). Through comprehensive database analysis, we found that miR-9-5p can act as a target miRNA for lncRNAs. Some researchers found that in an *in-vitro* model of myocardial infarction involving hypoxia-treated H9c2 cells, the levels of miR-9-5p were reduced (Cai *et al*., 2021). In a rat model of acute myocardial infarction, modulation of miR-9-5p using a specific agomir *in-vivo* effectively preserved cardiac function post-myocardial infarction while reducing fibrotic and inflammatory responses (Xiao *et al*., 2019).

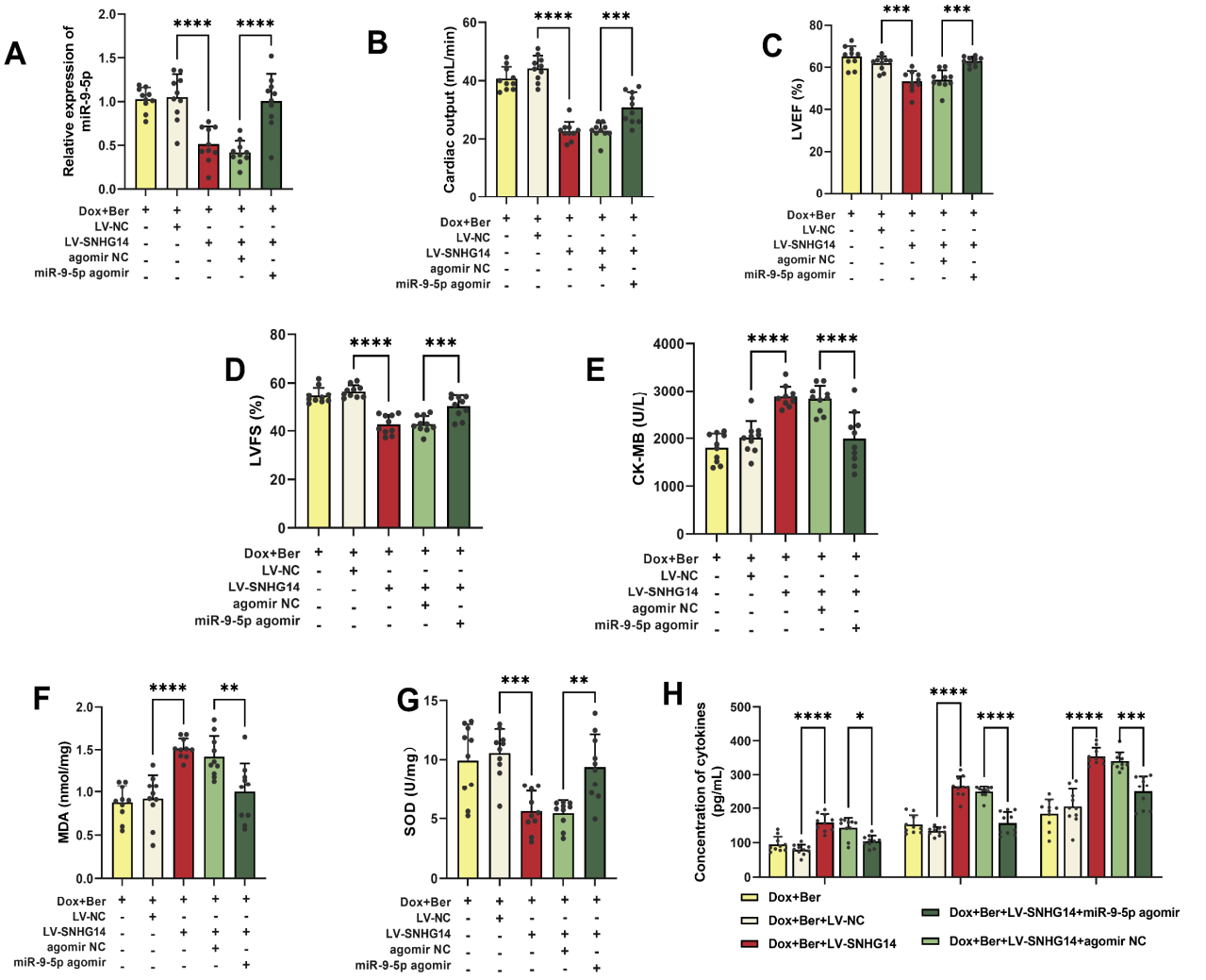

Fig. 6: MiR-9-5p partially reversed the elimination of the cardioprotective effect mediated by Ber due to SNHG14 *in-vivo*. (A) The levels of SNHG14 in myocardial tissues from rats were measured by conducting RT-qPCR; (B-D) Echocardiography was conducted to quantify cardiac output, LVEF, and LVFS; (E) The levels of CK-MB in rat serum were analyzed using a commercial kit; (F-G) The levels of MDA and SOD in myocardial tissues were examined by using commercial kits; (H) ELISA was performed to determine the levels of pro-inflammatory cytokines in the serum of the rats. The data were shown as mean ± SD, n = 10 rats/group, *$P < 0.05$, **$P < 0.01$, ***$P < 0.001$, ****$P < 0.0001$.

A recent study indicated that exosomes derived from pluripotent stem cells, which are derived from mesenchymal stem cells, effectively transported miR-9-5p into cardiomyocytes subjected to Dox treatment, thereby ameliorating myocardial damage (Zheng *et al*., 2024). Owing to the importance of miR-9-5p in myocardial injury, we focused our efforts on this miRNA. Our findings revealed that miR-9-5p directly interacts with SNHG14. The cardioprotective effect of SNHG14 against myocardial injury was significantly decreased by high levels of miR-9-5p. The main finding was that Ber may alleviate Dox-induced cardiotoxicity by inhibiting SNHG14/miR-9-5p.

By phosphorylating pyruvate dehydrogenase, PDK4 plays a role in metabolic regulation, contributing to the shift from mitochondrial respiration to cytoplasmic glycolysis, although it is not the primary driver of the Warburg effect. PDK4 plays a role in various types of cancer and several studies have focused on its role in resistance to chemotherapy. For example, miR-449 overexpression heightens the susceptibility of Dox-resistant triple-negative breast cancer cells to Dox (Torres-Ruiz *et al*., 2024).

Treatment with 0.5 μM Dox resulted in a notable increase in PDK4 mRNA levels, suggesting that PDK4 may be involved in the pathogenesis of Dox-triggered cardiac damage (Cunha-Oliveira *et al*., 2018). As shown in previous studies, our findings revealed that Dox induces the upregulation of PDK4 expression. We also made a novel discovery: Ber significantly impedes the increase in PDK4 levels caused by Dox, whereas the overexpression of SNHG14 significantly promotes PDK4 levels, but this promotion was significantly attenuated by miR-9-5p.

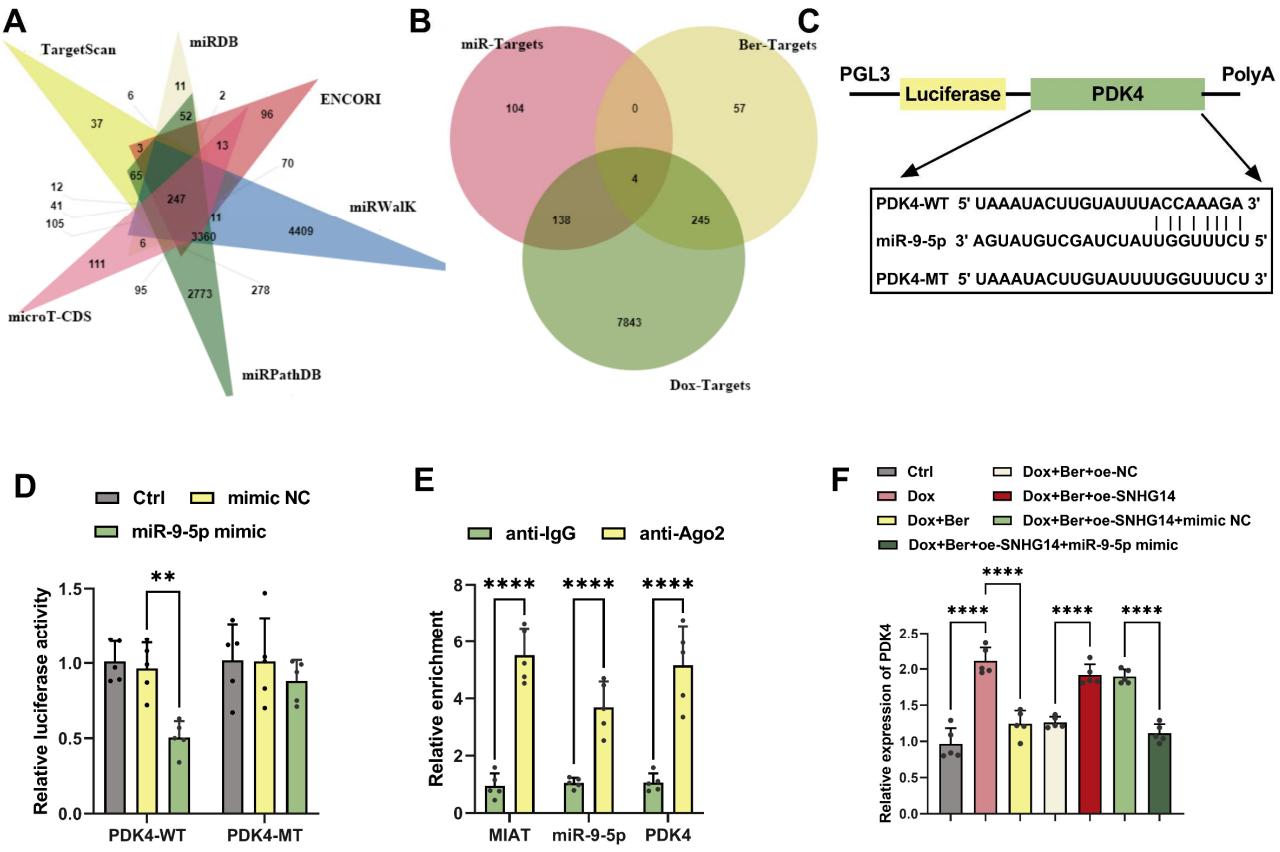

Fig. 7: PDK4 was a target of miR-9-5p. (A) The Venn diagram shows the overlapping target mRNAs of miR-9-5p predicted by the six databases. (B) The Venn diagram presents the common target mRNAs from miR-9-5p, Dox, and Ber. (C) Target binding sequences between PDK4 and miR-9-5p. (D-E) Dual luciferase reporter and RIP assays validated the targeting relationship between PDK4 and miR-9-5p. (F) RT-qPCR was performed to detect the effects of Dox, Ber, SNHG14, and miR-9-5p on PDK4 levels in AC16 cells. The data were shown as mean ± SD, n = 5 in each group, $^{**}P < 0.01$, $^{***}P < 0.001$, $^{****}P < 0.0001$.

Some studies have indicated that elevated expression of PDK can effectively reduce metabolic adaptability and aggravate cardiomyopathy; therefore, we suspected that Ber may further regulate metabolic levels through modulation of the SNHG14/miR-9-5p/PDK4 axis, affecting inflammation, oxidative stress and apoptosis, thereby mitigating Dox-induced cardiotoxicity, but this requires further validation. Limitations of this study restrict clinical applications, such as accumulation of 60 mg/kg over 10 days, which is a high dose for rats, with a risk of non-cardiac death. Although there were no extracardiac deaths in this study, the clinical long-term cumulative toxicity may be underestimated; dependence on functional/biochemical indices (e.g., CO, CK-MB) lacks pathological confirmation of myocardial injury. Moreover, the healthy male rat model does not fully replicate clinical patients with comorbidities, and the high-dose acute regimen may not reflect chronic low-dose cardiotoxicity. Future optimization of DOX dose (e.g., cumulative 15 mg/kg), longer observation period and inclusion of pathological analyses are necessary.

CONCLUSION

To summarize, a series of studies demonstrates that Ber alleviates Dox-induced cardiotoxicity by downregulating SNHG14 and disrupting the SNHG14/miR-9-5p/PDK4 axis, providing new therapeutic strategies for patients receiving Dox treatment.

Acknowledgments

None.

Authors' contributions

QYX and YHX: Conceptualization, methodology, formal analysis, investigation and writing-original draft preparation; HLH: Writing-review and editing.

Funding

There was no funding.

Data availability statement

The datasets generated during and/or analyzed during the current study are available from the corresponding author on reasonable request.

Ethical approval

The Research Ethics Committee of Chengdu University of Traditional Chinese Medicine (No.2018-01-0213) approved this study. This study was performed in adherence with the ARRIVE guidelines. See supplementary file for the ARRIVE checklist.

Conflict of interest

The authors declare no conflict of interest.

Supplementary data

https://www.pjps.pk/uploads/2026/07/SUP1784551067.pdf

REFERENCES

El-Aziz AA, El-Desouky MA, Shafei A, Elnakib M and Abdelmoniem AM (2021). Influence of pentoxifylline on gene expression of PAG1/ miR-1206/ SNHG14 in ischemic heart disease. *Biochem Biophys Rep,* **25**: 100911.

Ahmedy OA, Salem HH, Mohamed YS and Zaky DA (2025). Unleashing the cardioprotective potential of berberine against doxorubicin cardiotoxicity: Innovative exploitation of the peculiar antipyroptotic/antioxidant/anti-inflammatory capacity via modulation of inflammasome/caspase-1/interleukin pathway in rats. *Int Immunopharmacol,* **159**: 114964.

Alruhaimi RS, Abduh MS, Ahmeda AF, Bin-Ammar A, Kamel EM, Hassanein EHM, Li C and Mahmoud AM (2024). Berberine attenuates inflammation and oxidative stress and modulates lymphocyte E-NTPDase in acute hyperlipidemia. *Drug Dev Res,* **85**(2): e22166.

Bi C, Wang D, Hao B and Yang T (2024). Snhg14/miR-181a-5p axis-mediated "M1" macrophages aggravate LPS-induced myocardial cell injury. *Heliyon,* **10**(18): e37104.

Cai X, Li B, Wang Y, Zhu H, Zhang P, Jiang P, Yang X, Sun J, Hong L and Shao L (2021). CircJARID2 Regulates Hypoxia-Induced Injury in H9c2 Cells by Affecting miR-9-5p-Mediated BNIP3. *J Cardiovasc Pharmacol.,* **78**(1): e77-e85.

Chen B and Zhang JP (2022). Bcl-xL is required for the protective effects of low-dose berberine against doxorubicin-induced cardiotoxicity through blocking apoptosis and activating mitophagy-mediated ROS elimination. *Phytomedicine,* **101**: 154130.

Chen L and Mao Y (2024). Berberine inhibits the glycolysis and proliferation of hepatocellular carcinoma cells by down-regulating HIF-1alpha. *Pak J Pharm Sci,* **37**(6): 1351-1363.

Chen Z, Liu Y, Ma R, Zhang M, Wu X, Pen H, Gui F, Liu Y, Xia H, Hu N, Ai B, Xiong J, Xia H, Li W and Ai F (2024). Protective effect of long noncoding RNA OXCT1-AS1 on doxorubicin-induced apoptosis of human myocardial cells by the competitive endogenous RNA Pattern. *Arq Bras Cardiol.,* **121**(6): e20230675.

Oliveira TC, Ferreira LL, Coelho AR, Deus CM and Oliveira PJ (2018). Doxorubicin triggers bioenergetic failure and p53 activation in mouse stem cell-derived cardiomyocytes. *Toxicol Appl Pharmacol.,* **348**: 1-13.

Du C, Deng Rb, Li J and Wang YF (2025). Anti-cancer effects of Trifolium pratense L. on hepatocellular carcinoma via the HOTAIR/miR-124/Notch1 pathway: A biochemical and histopathological study in rats. *Pak J Pharm Sci,* **38**(3): 945-957.

Fujii K, Fujiwara-Tani R, Nukaga S, Ohmori H, Luo Y, Nishida R, Sasaki T, Miyagawa Y, Nakashima C, Kawahara I, Ogata R, Ikemoto A, Sasaki R and Kuniyasu H (2024). Involvement of Ferroptosis induction and oxidative phosphorylation inhibition in the anticancer-drug-induced myocardial injury: ameliorative role of pterostilbene. *Int J Mol Sci.,* **25**(5): 3015.

Guan X, Wang Y, Li W, Liu X, Jiang J, Bian W, Xu C, Sun Y and Zhang C (2023). The effects and mechanism of LncRNA NORAD on doxorubicin-induced cardiotoxicity. *Toxicology,* **494**: 153587.

Han Y, Guo S, Li Y, Li J, Zhu L, Liu Y, Lv Y, Yu D, Zheng L, Huang C, Li C, Hu J and Liu Z (2023). Berberine ameliorate inflammation and apoptosis via modulating PI3K/AKT/NFkappaB and MAPK pathway on dry eye. *Phytomedicine,* **121**: 155081.

Huang Q, Qiu T, Chen H, Tian T, Wang D and Lu C (2025). Silencing LncRNA SNHG14 alleviates renal tubular injury via the miR-483-5p/HDAC4 axis in diabetic kidney disease. *Hormones (Athens),* **24**(1): 123-135.

Jia X, Shao W and Tian S (2022). Berberine alleviates myocardial ischemia-reperfusion injury by inhibiting inflammatory response and oxidative stress: The key function of miR-26b-5p-mediated PTGS2/MAPK signal transduction. *Pharm Biol.,* **60**(1): 652-663.

Jiang H, Ni J, Zheng Y and Xu Y (2021). Knockdown of lncRNA SNHG14 alleviates LPS-induced inflammation and apoptosis of PC12 cells by regulating miR-181b-5p. *Exp Ther Med,* **21**(5): 497.

Li C, Jiang S, Wang H, Wang Y, Han Y and Jiang J (2022). Berberine exerts protective effects on cardiac senescence by regulating the Klotho/SIRT1 signaling pathway. *Biomed Pharmacother,* **151,** 113097.

Linders AN, Dias IB, López Fernández T, Tocchetti CG, Bomer N, and Van der Meer P (2024). A review of the pathophysiological mechanisms of doxorubicin-induced cardiotoxicity and aging. *NPJ Aging,* **10**(1): 9.

Long Y, Wang L and Li Z (2020). SP1-induced SNHG14 aggravates hypertrophic response in *in vitro* model of cardiac hypertrophy via up-regulation of PCDH17. *J Cell Mol Med,* **24**(13): 7115-7126.

Lu G, Cheng Z, Wang S, Chen X, Zhu X, Ge Z, Wang B, Sun J, Hu J and Xuan J (2021). Knockdown of Long Noncoding RNA SNHG14 Protects H9c2 Cells Against Hypoxia-induced Injury by Modulating miR-25-3p/KLF4 Axis *in vitro*. *J Cardiovasc Pharmacol,* **77**(3): 334-342.

Ma H, Xing C, Wei H, Li Y, Wang L, Liu S, Wu Q, Sun C and Ning G (2024). Berberine attenuates neuronal ferroptosis via the AMPK-NRF2-HO-1-signaling pathway in spinal cord-injured rats. *Int Immunopharmacol,* **142**(Pt B): 113227.

Mu Y, Geng J, Liu C, Jiang S, Han Y, Jiang J and Wang Y (2025). Exploring the multi-faceted effects of berberine in ameliorating diastolic dysfunction in rats with heart failure with preserved ejection fraction. *Int J Mol Sci,* **26**(10): 4747.

Rawal S, Gupta P, Bhatnagar P, Yadav HN and Dinda AK (2022). Solid lipid nanoformulation of berberine attenuates doxorubicin triggered *in vitro* inflammation in H9c2 Rat cardiomyocytes. *Comb Chem High Throughput Screen,* **25**(10): 1695-1706.

Tian J and Zhang D (2025). Periplocin has anti-tumor actions in prostate cancer through modulating the miR-3614-5p/SLC4A4 axis. *Pak J Pharm Sci,* **38**(4): 1309-1320.

Torres-Ruiz S, Garrido-Cano I, Lameirinhas A, Burgués O, Hernando C, Martínez MT, Rojo F, Bermejo B, Tapia M, Carbonell-Asins JA, Peña CJ, Lluch A, Cejalvo JM, Tormo E and Eroles P (2024). MiRNA-449 family is epigenetically repressed and sensitizes to doxorubicin through ACSL4 downregulation in triple-negative breast cancer. *Cell Death Discov,* **10**(1): 372.

Wang Y, Liao J, Luo Y, Li M, Su X, Yu B, Teng J, Wang H and Lv X (2023). Berberine alleviates doxorubicin-induced myocardial injury and fibrosis by eliminating oxidative stress and mitochondrial damage via promoting Nrf-2 pathway activation. *Int J Mol Sci,* **24**(4): 3257.

Wei G, Liu B, Guo Y, Qiu W, Lei X, Li J, Yin H, Liang L and Lv M (2025). LINC01106 stimulates growth and metastasis of colorectal carcinoma by sponging miR-744-5p. *Pak J Pharm Sci,* **38**(4): 1378-1388.

Wu YZ, Zhang L, Wu ZX, Shan TT and Xiong C (2019). Berberine Ameliorates Doxorubicin-induced cardiotoxicity via a SIRT1/p66Shc-mediated pathway. *Oxid Med Cell Longev,* 2019: 2150394.

Xiao Y, Zhang Y, Chen Y, Li J, Zhang Z, Sun Y, Shen H, Zhao Z, Huang Z, Zhang W, Chen W and Shen Z (2019). Inhibition of MicroRNA-9-5p Protects against cardiac remodeling following myocardial infarction in mice. *Hum Gene Ther,* **30**(3): 286-301.

Xu F, Bian N and Li X (2024). SNHG14 Elevates NFAT5 Expression through sequestering miR-375-3p to promote MPP + -induced neuronal apoptosis, inflammation and oxidative stress in parkinson's disease. *Neurochem Res,* **49**(5): 1212-1225.

Yang Y, Jiang S, Mu Y, Liu C, Han Y, Jiang J, Wang Y (2024). Berberine prevents against myocardial injury induced by acute beta-adrenergic overactivation in rats. *J Appl Toxicol,* **44**(11): 1700-1713.

Zhai X, Zhou J, Huang X, Weng J, Lin H, Sun S, Chi J, Meng L (2024). LncRNA GHET1 from bone mesenchymal stem cell-derived exosomes improves doxorubicin-induced pyroptosis of cardiomyocytes by mediating NLRP3. *Sci Rep,* **14**(1): 19078.

Zhang G, Li T, Chang X and Xing J (2021a). Long noncoding RNA SNHG14 promotes ischemic brain injury via regulating miR-199b/AQP4 Axis. *Neurochem Res,* **46**(5): 1280-1290.

Zhang Q, Liu J, Duan H, Li R, Peng W and Wu C (2021b). Activation of Nrf2/HO-1 signaling: An important molecular mechanism of herbal medicine in the treatment of atherosclerosis via the protection of vascular endothelial cells from oxidative stress. *J Adv Res,* **34**: 43-63.

Zheng D, Xiao W, Duan D, Tang C and Lin X (2025a). Effectiveness of emotional freedom techniques therapy in alleviating anticipatory grief for cancer patients. *Medicine (Baltimore),* **104**(36): e44211.

Zheng H, Liang X, Liu B, Huang X, Shen Y, Lin F, Chen J, Gao X, He H, Li W, Hu B, Li X, Zhang Y (2024). Exosomal miR-9-5p derived from iPSC-MSCs ameliorates doxorubicin-induced cardiomyopathy by inhibiting cardiomyocyte senescence. *J Nanobiotechnology,* **22**(1): 195.

Zheng Y, Kou J, Gao X, Guo J, Liu Q, Ren H, Gao T, Wang Q, Zhao Y, Wang Y, Li H and Yang L (2025b). Berberine inhibited SASP-related inflammation through RXRalpha/PPARgamma/NEDD4 pathway in atherosclerosis. *Am J Chin Med,* **53**(1): 251-283.

Zhu Y, Wang Y, Xing S and Xiong J (2021). Blocking SNHG14 antagonizes lipopolysaccharides-induced acute lung injury via SNHG14/miR-124-3p Axis. *J Surg Res,* 263:140-150.

Zou R, Wang S, Cai H, Wang Y and Wang C (2023). Pharmacological activation of rev-erbalpha attenuates doxorubicin-induced cardiotoxicity by PGC-1alpha signaling pathway. *Cardiovasc Ther,* 2023: 2108584.